

## Evaluation of Calcined Hydrocalumite-type Materials as Supports of CoMo and NiMo for Thiophene Hydrodesulfuration Reaction

Carlos Felipe Linares<sup>a\*</sup>, Pablo Bretto<sup>a</sup>, Ruth Álvarez<sup>a</sup>, Freddy Ocanto<sup>a</sup>,

Carolina Corao<sup>a</sup>, Paulino Betancourt<sup>b</sup>, Joaquín Luis Brito<sup>c</sup>

<sup>a</sup>Departamento de Química, Facultad de Ciencias y Tecnología, Unidad de Síntesis de Materiales y Metales de Transición, Universidad de Carabobo, Valencia. Edo. Carabobo, Venezuela

<sup>b</sup>Laboratorio de Tratamiento Catalítico de Efluentes, Centro de Catálisis, Petróleo y Petroquímica, Universidad Central de Venezuela. Caracas, Venezuela

<sup>c</sup>Laboratorio de Físicoquímica de Superficies, Centro de Química, Instituto Venezolano de Investigaciones Científicas, IVIC. Apartado 20632, Caracas 1020-A, Venezuela

Received: August 28, 2013; Revised: January 28, 2014

A hydrocalumite-type material (HC) was synthesized by the co-precipitation method, mixing Ca and Al nitrate solutions in a NaOH solution (pH  $\cong$  11). This solid was characterized by using different physico-chemical techniques such as: Fourier-transform infrared spectroscopy (FT-IR), X-ray diffraction (XRD), temperature programmed reduction (TPR) and BET surface area measurements. Then, a portion of as-synthesized solid was calcined at 420 °C (HC 420). Both calcined and pristine solids were impregnated with Mo (15% w/w as MoO<sub>3</sub>). Ni or Co was also impregnated on Mo/HC or Mo/HC 420 in 1(Co or Ni):3 (Mo) atomic ratios to get catalytic precursors. These solids were also characterized by the above mentioned techniques. Catalytic precursors were tested in the thiophene hydrodesulfuration reaction at 280 °C and atmospheric pressure. Cobalt promoted catalysts were more active than those promoted with Ni. However, thiophene conversions were lower than that of a conventional CoMo/ $\gamma$ -Al<sub>2</sub>O<sub>3</sub> catalyst.

**Keywords:** hydrocalumite, hydrotreatment, thiophene, CoMo, NiMo

### 1. Introduction

Hydrotreatment (HDT) is often used for reducing heteroatoms and aromatics contents from fossil fuels. Therefore, HDT catalysts play a very important role, both in refining technology and for environment protection. Effectiveness of these catalysts minimizes costs of production of clean combustibles<sup>1,2</sup>.

New legislations have been advanced in order to impose minimum sulfur contents in fossil fuels. A possibility to produce better catalysts is the use of new supports which should render more active and cheaper catalysts than those currently employed<sup>3</sup>.

In this way, hydrotalcite-type materials, whose structure is similar to hydrocalumite-types, have been studied as HDT catalyst supports, especially, those synthesized with Al and Mg<sup>4,5</sup>; however, Ca-Al hydrocalumite-type solids have not been documented for this purpose. Hydrotalcites and hydrocalumite are two minerals closely related, belonging to the layered double hydroxide family. Both structures are based on positive brucite-like layers alternating with layers containing anions and water molecules. Hydrotalcites-like materials are far more common, while hydrocalumite structure type is rare and less broad in composition<sup>4,5</sup>.

Vieille et al.<sup>6</sup>, studied the phases obtained upon dehydration and decomposition of hydrocalumites by using

different techniques such as *in situ* (high temperature) XRD and TGA. TGA analysis showed that this type of solid undergoes to three-step decomposition on heating: dehydration, dehydroxylation, and anion expulsion, respectively, over the following temperature ranges: 25-250, 250-400, and >400 °C. Sharp phase transitions were observed as a result of the ordered distribution of Ca and Al atoms in the hydroxide layer and the well-ordered interlayer structure.

On the other hand, López-Salinas et al.<sup>7</sup>, studied hydrocalumites in the isomerization reaction of 1-butene. This solid was characterized by XRD, surface area and pore size and CO<sub>2</sub> TPD. The layered structure of HC collapses above 250°C yielding an amorphous material at 323°C, which upon calcination at 600-700°C transforms into a mixture of CaO and mayenite (calcium aluminium oxide of cubic symmetry, Ca<sub>12</sub>Al<sub>14</sub>O<sub>33</sub>). The calcination temperature has a marked effect in the formation of basic sites. Thus for example, HC calcined at 800°C shows 90% of strong basic sites while they are absent in HC calcined at 600-700°C.

This paper explores the hydrocalumite as support of CoMo or NiMo oxides for use in the HDS reaction of thiophene. Results were compared to a commercial CoMo/alumina catalyst.

\*e-mail: [clinares@uc.edu.ve](mailto:clinares@uc.edu.ve)



On the other hand, a wide band placed between 3500 and 3600  $\text{cm}^{-1}$  and a low band at 1646  $\text{cm}^{-1}$  observed in HC 420 correspond to water molecules physisorbed on the HC 420 surface.

A broad band placed around 1446  $\text{cm}^{-1}$  is due to carbonate species which should be different from those existing in hydrocalumite<sup>9</sup>. These carbonate species could be associated to formation of surface  $\text{CaCO}_3$  due to exposure to an air atmosphere (atmospheric  $\text{CO}_2$  and humidity) and basicity of solid<sup>11</sup>. A main band at 834  $\text{cm}^{-1}$ , absent in the spectrum of hydrocalumite, and a broad band around 550  $\text{cm}^{-1}$ , are due to the major changes originated by the phase transformations during the calcination process. They are due to metal-oxygen bonds<sup>9</sup>.

By examining the results of Vieille et al.<sup>6</sup>, López-Salinas et al.<sup>7</sup> and Campos-Molina et al.<sup>12</sup>, it can be concluded that the transformation of hydrocalumite during the calcination occurs in three steps: in the first one (25-200°C), the physisorbed water is lost from the hydrocalumite structure. The second (200-400°C) and third steps (400-800°C) correspond to dehydroxylation and expulsion of anions. An exact sequence has not been established, however, it was reported that the material still loses water from dehydroxylation at temperatures above 600°C<sup>12</sup>. This could explain water molecule bands of the material observed on HC 420 (Figure 1b).

A clear identification of hydrocalumite phases was done by using XRD. Figure 2 shows the XRD pattern of HC and HC 420.

Characteristic intense peaks at 10, 20 and 29 degrees (2 $\theta$ ), and also other less intense bands belonging to HC<sup>6</sup> were found in the corresponding sample; moreover, a small amount  $\text{CaCO}_3$  phase (JCPDS: 85-1108) could be also identified. The basic conditions of synthesis of hydrocalumite, permitted the formation  $\text{CaCO}_3$  due to absorption of atmospheric  $\text{CO}_2$ .

The calcination of HC produced the formation of different phases such as: CaO (JCPDS: 17-0912),  $\text{Ca}_{12}\text{Al}_{14}\text{O}_{33}$  mayenite (JCPDS: 48-1882) and  $\text{CaCO}_3$  (JCPDS: 85-1108) (Figure 2). According to López-Salinas et al.<sup>7</sup>, the calcination of HC at 500°C produces CaO, while calcination at higher temperatures (upon 600°C) produces CaO and  $\text{Ca}_{12}\text{Al}_{14}\text{O}_{33}$ .

BET surface area measurements were also carried out. One can see that for HC 420 (17  $\text{m}^2/\text{g}$ ), the surface area is diminished in 23% in comparison with that of HC (22  $\text{m}^2/\text{g}$ ). This could be associated to the higher size of crystallites. López-Salinas et al.<sup>7</sup>, showed that calcination of HC between 400-500°C produced surface areas between 34-26  $\text{m}^2/\text{g}$ , in agreement with the lower crystallinity of their solids.

Figure 3 shows the XRD patterns of CoMo/(HC or HC 420) catalytic precursors. Several oxidic phases such as  $\text{MoO}_3$  (JCPDS: 85-2405), scheelite  $\text{CaMoO}_4$  (JCPDS: 85-1267), CaO (JCPDS: 17-0912), mayenite  $\text{Ca}_{12}\text{Al}_{14}\text{O}_{33}$  (JCPDS: 48-1882) and  $\text{CaCO}_3$  (JCPDS: 85-1108) were identified.

$\text{MoO}_3$  is produced by oxidation of the impregnated molybdenum precursor. Phases containing Co oxides were not detected for CoMo/(HC or HC 420). This result could be due to the low Co concentration or to Co oxide crystals

being amorphous. Similar results were obtained for NiMo/(HC or HC 420). (Figure 4)

XRD patterns of CoMo and NiMo supported on HC or HC 420 were quite similar. Therefore, from this technique point of view there are not differences due to the additional calcination procedure.

Table 1 shows the BET surface areas measurements of studied catalytic precursors. An increase of BET surface area from 38 to 43  $\text{m}^2/\text{g}$  was observed when comparing CoMo/HC with CoMo/HC 420. In similar way, for NiMo/HC 420 was observed an increase of 37 % with respect to NiMo/HC.

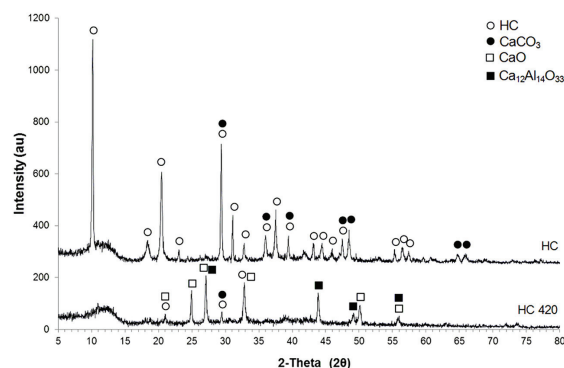


Figure 2. Powder XRD patterns of HC and HC 420.

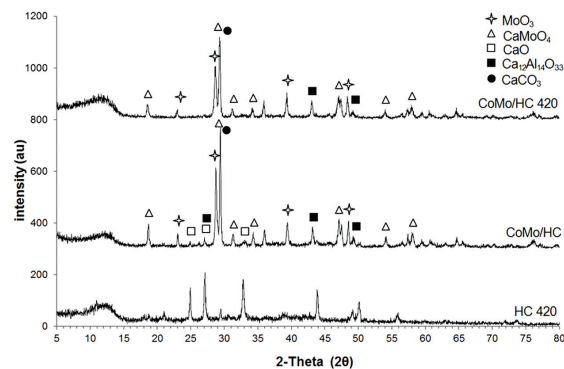


Figure 3. Powder XRD patterns of CoMo catalytic precursors supported on HC and HC 420.

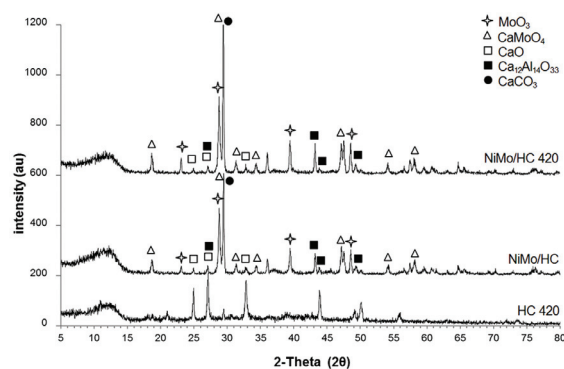


Figure 4. Powder XRD patterns of NiMo catalytic precursors supported on HC and HC 420.

It could be speculated that micropores could be obtained in the supported oxide phases (see below).

Comparing the BET surface area of solids, HC and HC 420, and those reported on Table 1, we can observe that the BET surface area of HC is decreased when the support is calcined. The decrease in surface area of HC upon increasing calcination temperature (below 300°C) is opposite to the behavior of hydrotalcite<sup>13,14</sup>. According to López-Salinas et al.<sup>7</sup>, mesopore diameter of HC is increased as the calcination temperature increases which could decrease the BET surface area. Moreover, the expulsion of anions and water from HC and the formation of a dense phase could also decrease the BET surface area in these solids.

On the contrary, the surface area of supported oxides is increased when these are calcined. Impregnated oxides (CoMoO<sub>x</sub> and NiMoO<sub>x</sub>) or mixed phases formed with the hydrocalumite components (CaMoO<sub>4</sub>) could produce a microporous surface structure on the HC phase.

The nature of molybdenum and cobalt species on HC and HC 420 was determined from the TPR profiles. For CoMo/HC catalyst (Figure 5) it was observed a complex pattern consisting of three peaks. The first one, of low intensity and located between 300 and 400°C, could be ascribed to partial reduction of a small amount of octahedral polymeric molybdenum species whose reducibility is increased by the promoter as compared to unpromoted polymolybdates<sup>15-17</sup>. This TPR peak has been correlated to the catalytic activity displayed by promoted, molybdena-based catalysts<sup>16,17</sup>. An intermediate temperature signal between 450 and 700°C

could include further reduction of the above species plus the partial reduction of additional unpromoted octahedral supported phases, and of tetrahedral Mo species from CaMoO<sub>4</sub>. It is worth mentioning that TPR peaks of alkali and alkali-earth metal molybdates appear at higher temperatures (usually above 700°C), and that they have been found to be incompletely reduced under the dynamic conditions of TPR at temperatures well in excess of 1000°C<sup>18-21</sup>. However, the presence of Ni and Co helps in attaining higher rates (TPR peaks at lower temperatures) and extents of reduction (more intense peaks) of these phases<sup>22,23</sup>. Finally, a wide signal between 800 and 1000°C could be a combination of the further reduction up to Mo metal of all molybdena containing phases plus that of the spinel-like phases of the promoters Co (and Ni) associated to the support. It is possible, however, that the reduction is not completed at the highest temperature of the present experiments.

Likewise, CoMo/HC 420 showed also three reduction zones (Figure 5), the main difference being that the first one corresponding to promoted octahedral polymeric molybdenum species was less pronounced than CoMo/HC and slightly shifted to higher temperatures, suggesting decreased reducibility, which could be due to loss of the promoter from the surface by reaction with the support during calcination. The rest of reduction zones were quite similar to CoMo/HC.

Previous studies have shown that the lower temperature peaks of unsupported NiMoO<sub>4</sub><sup>22</sup> as well as Ni promoted Mo-based catalysts supported on alumina<sup>15</sup>, silica<sup>16</sup> or silica-alumina<sup>22</sup>, among other materials, appear always at lower temperatures than the corresponding Co containing solids. Thus, it is striking that the catalysts prepared in the present study show the opposite behavior, i.e., the intensities of the first signal assigned to promoted polymolybdates are lower and the peak temperatures of the same signals are higher for Ni promoted samples (Figure 5). For the second peak there is also decreased intensity of the Ni containing catalysts at the lower temperature side of the peaks. This could be interpreted as due to Ni ions being interacting strongly with calcium oxides from the support, and thus being less available to increase the reducibility of supported polymolybdates. As in the case of the CoMo samples, the second and third peaks of the reductograms do not show significant differences between NiMo/HC and NiMo/HC 420.

Figure 6 shows the catalytic behavior of CoMo and NiMo supported on HC or HC 420. A CoMo commercial catalyst was tested for comparison. As can be seen, the commercial catalyst was more active than CoMo and NiMo supported on HC and HC 420.

Initially (15-30 min of time on stream) the CoMo/HC conversion was 40%. Then, this value dropped down to a 2.5% conversion at 85 min of reaction time and kept essentially constant up to 240 min. On the other hand, CoMo/HC 420 showed a very low conversion (~0.9%) during the full range of reaction time.

In order to better compare the activities of the samples, it was calculated the catalytic activity of catalysts determined as: converted thiophene moles/(time\*surface area) (Table 2). It can be seen that the CoMo/HC catalysts

**Table 1.** BET surface area of catalytic precursors.

Samples	BET surface area (m <sup>2</sup> /g)
CoMo/HC	38
CoMo/HC 420	43
NiMo/HC	43
NiMo/HC 420	59

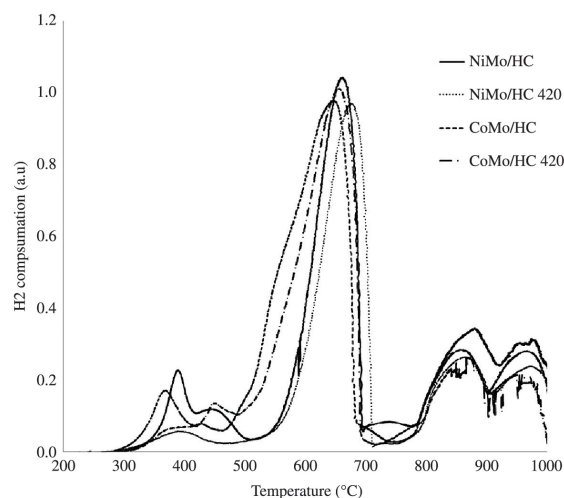


**Figure 5.** TPR profile of CoMo and NiMo supported on HC or HC 420.

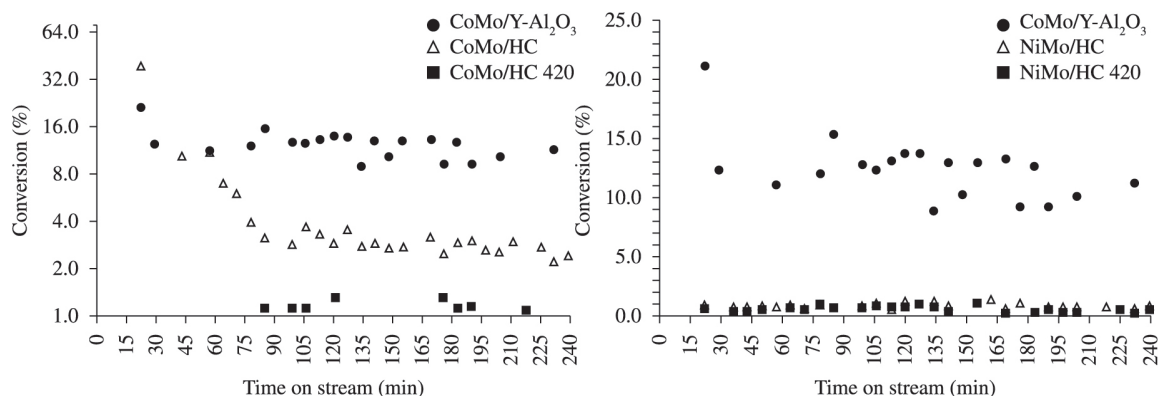


**Figure 6.** Thiophene conversion on a commercial CoMo/ $\gamma$ -Al<sub>2</sub>O<sub>3</sub> catalyst and NiMo (a) or CoMo (b) supported on HC and HC 420.

**Table 2.** Catalytic activity of the thiophene HDS reaction in presence of synthesized Co(Ni)Mo/(HC or HC420) catalysts.

Samples	Activity x 10 <sup>-10</sup> (Converted thiophene moles/(s.m <sup>2</sup> ))
CoMo/ $\gamma$ -alumina	6.57
CoMo/HC	7.22
CoMo/HC 420	1.80
NiMo/HC	2.10
NiMo/HC 420	0.92

shows a higher activity than the commercial catalyst. This result demonstrates that the intrinsic activity of the active sites of the CoMo/HC supported sample are quite similar or even higher than that of sites of the commercial catalyst.

Figure 6 shows the catalytic behavior of NiMo/HC and NiMo/HC 420. Both catalysts showed a very small thiophene conversion during the whole reaction time (~0.9 % and ~0.7 % respectively). Their activity calculated in terms of the surface area (Table 2) is also lower for NiMo samples than for the CoMo ones, which again could be the result of the higher interaction of Ni promoter with the HC support as compared with Co.

Calcination effect (after and before impregnation) did not show a marked effect on the thiophene conversion for most of these catalysts, although in both cases the activity of phases supported on HC is higher than on HC-420. As the active phases of both promoted and unpromoted Mo catalysts consist of sulfides of the metals, mainly Mo, it can be assumed that the interaction with HC and the other phases observed (e.g., scheelite), render the Mo-containing phases very difficult to be sulfided, as was confirmed in TPR profiles. In particular, alkali and alkaline-earth metal molybdates have been shown to be much less reducible (and thus, probably less sulfidable) than MoO<sub>3</sub> and/or mixed Co- and Ni-molybdates<sup>18-21</sup>. However, for CoMo catalyst supported on non calcined HC the conversion was very high at the start of reaction and kept higher at the end than that on the calcined support. Probably in this instance, the interaction between the supported phases and the HC

support was lower, allowing the initial formation of the active sulfides, which suffer a slow reorganization with time, leading to the final observed conversion. Likewise, TPR profiles confirmed that CoMo/HC catalysts should be more active than those CoMo/HC-420 catalysts because they showed a higher presence of octahedral, promoted Mo species.

BET surface area did not play an important role between synthesized catalysts. The catalytic activity was quite similar among catalytic precursors of similar composition (Table 2). However, CoMo/HC catalysts, whose surface area was lower than CoMo/HC-420, 38 vs 43 m<sup>2</sup>/g, showed a higher activity. This result could be associated again to a less strong interaction between the metal promoter and support in the case of the uncalcined support.

Thus, the low observed conversions in Figure 6 could be associated to the low surface area shown by these catalysts. Moreover, hydrocalumites have showed a basic behavior, where basic sites strength increases with the calcination temperature<sup>7</sup> and which could influence the activity for the HDS reaction.

#### 4. Conclusions

Hydrocalumite was synthesized and characterized by different techniques such as FT-IR and XRD. These analyses showed the formation of CaCO<sub>3</sub> as a collateral phase. When hydrocalumite was calcined, different phases such as CaO and mayenite (Ca<sub>12</sub>Al<sub>14</sub>O<sub>33</sub>) were obtained. CoMo and NiMo supported on HC, before and after calcination, showed a conversion generally negligible in thiophene HDS reaction. These results could be associated to strong interaction of the supported Mo and Co/Ni oxides with the HC and/or Ca oxides phases, to the low surface area or to the strong basicity showed by these catalysts.

#### Acknowledgements

We are grateful to Fonacit (PAE-FONACIT N° 2011000797) for funding the research carried out in this work.

## References

1. Rana M, Sámano V, Ancheyta J and Díaz JAI. A review of recent advances on process technologies for upgrading of heavy oils and residua. *Fuel*. 2007; 86(9):1216-1231. <http://dx.doi.org/10.1016/j.fuel.2006.08.004>
2. Kibby CL and Swift HE. Study of catalysts for ciclohexane-thiophene transfer reaction. *Journal of Catalysis*. 1976; 45(2):231-241. [http://dx.doi.org/10.1016/0021-9517\(76\)90137-8](http://dx.doi.org/10.1016/0021-9517(76)90137-8)
3. Marcilly C. Evolution of refining and petrochemicals. What is the place of zeolites. *Studies in Surface Science and Catalysis*. 2001; 135:37-60. [http://dx.doi.org/10.1016/S0167-2991\(01\)81185-X](http://dx.doi.org/10.1016/S0167-2991(01)81185-X)
4. Caloch B, Rana S and Ancheyta J. Improved hydrogenolysis (C-S, C-M) function with basic supported hydrodesulfurization catalysts. *Catalysis Today*. 2004; 98(1-2):91-98. <http://dx.doi.org/10.1016/j.cattod.2004.07.023>
5. Álvarez R, Tóffolo A, Pérez V and Linares CF. Synthesis and characterization of CoMo/Zn-Al mixed oxide catalysts for hydrodesulfurization of thiophene. *Catalysis Letters*. 2010; 137(3-4):150-155. <http://dx.doi.org/10.1007/s10562-010-0337-9>
6. Vieille L, Rousselot I, Leroux F, Besse JP and Taviot-Guého C. Hydrocalumite and its polymer derivatives. 1. Reversible thermal behavior of Friedel's salt: a direct observation by means of high-temperature in situ powder X-ray diffraction. *Chemistry of Materials*. 2003; 15(23):4361-4368. <http://dx.doi.org/10.1021/cm031069j>
7. López-Salinas E, Llanos ME, Cortés MA and Schifter I. Characterization of synthetic hydrocalumite [Ca<sub>2</sub>Al(OH)<sub>6</sub>]NO<sub>3</sub>.mH<sub>2</sub>O: effect of the calcination temperature. *Journal of Porous Materials*. 1995; 2(4):291-297. <http://dx.doi.org/10.1007/BF00489810>
8. Kok K-H, Lim T-T and Dong Z. Application of layered double hydroxides for removal of oxyanions: a review. *Water Research*. 2008; 42(6-7):1343-1368. PMID:18061644. <http://dx.doi.org/10.1016/j.watres.2007.10.043>
9. Palmer SJ, Frost RL and Nguyen T. Hydrotalcites and their role in coordination of anions in Bayer liquors: anion binding in layered double hydroxides. *Coordination Chemistry Reviews*. 2009; 253(1-2):250-267.
10. Reis MJ, Silveiro F, Tronto J and Valim JB. Effects of pH, temperature, and ionic strength on adsorption of sodium dodecylbenzenesulfonate into Mg-Al-CO<sub>3</sub> layered double hydroxides. *Journal of Physics and Chemistry of Solids*. 2004; 65(2-3):487-492.
11. Domínguez M, Pérez-Bernal ME, Ruano-Casero RJ, Barriga C, Ferreira R, Carlos LD et al. Multiwavelength luminescence in lanthanide-doped hydrocalumite and mayenite. *Chemistry of Materials*. 2011; 23(7):1993-2004. <http://dx.doi.org/10.1021/cm200408x>
12. Campos-Molina M, Santamaría-González J, Mérida-Robles J, Moreno-Tost R, Alburquerque M, Bruque-Gámez S et al. Base catalysts derived from hydrocalumite for the transesterification of Sunflower oil. *Energy Fuels*. 2009; 24(2):979-984. <http://dx.doi.org/10.1021/ef9009394>
13. Reichle WT, Kang SY and Everhardt DS. The nature of the thermal decomposition of a catalytically active anionic clay mineral. *Journal of Catalysis*. 1986; 101(2):352-359. [http://dx.doi.org/10.1016/0021-9517\(86\)90262-9](http://dx.doi.org/10.1016/0021-9517(86)90262-9)
14. Schaper H, Berg-Slot JJ and Stork WHJ. Stabilized magnesia: a novel catalyst (support) material. *Applied Catalysis*. 1989; 54(1):79-90. [http://dx.doi.org/10.1016/S0166-9834\(00\)82356-8](http://dx.doi.org/10.1016/S0166-9834(00)82356-8)
15. Brito JL and Laine J. Reducibility of Ni-Mo/Al<sub>2</sub>O<sub>3</sub> catalysts: a TPR study. *Journal of Catalysis*. 1993; 139(2):540-550. <http://dx.doi.org/10.1006/jcat.1993.1047>
16. Laine J, Brito JL and Severino F. Structure and activity of NiCoMo/SiO<sub>2</sub> hydrodesulfurization catalysts. *Journal of Catalysis*. 1991; 131(2):385-393. [http://dx.doi.org/10.1016/0021-9517\(91\)90273-7](http://dx.doi.org/10.1016/0021-9517(91)90273-7)
17. Burch R and Collins A. Temperature-programmed reduction of Ni/Mo hydrotreating catalysts. *Applied Catalysis*. 1985; 18(2):389-400. [http://dx.doi.org/10.1016/S0166-9834\(00\)84015-4](http://dx.doi.org/10.1016/S0166-9834(00)84015-4)
18. Zhang YJ, Rodríguez-Ramos I and Guerrero-Ruiz A. Oxidative dehydrogenation of isobutane over magnesium molybdate catalysts. *Catalysis Today*. 2000; 61(1-4):377-382. [http://dx.doi.org/10.1016/S0920-5861\(00\)00398-9](http://dx.doi.org/10.1016/S0920-5861(00)00398-9)
19. Driscoll SA, Gardner DK and Ozkan US. Characterization, activity, and adsorption/desorption behavior alkali-promoted molybdate catalysts for the oxidative coupling of methane. *Journal of Catalysis*. 1994; 147(2):379-392. <http://dx.doi.org/10.1006/jcat.1994.1156>
20. Erdöhelyi A, Maté F and Solymosi F. Partial oxidation of ethane over silica-supported alkali metal molybdate catalysts. *Journal of Catalysis*. 1992; 135(2):563-575. [http://dx.doi.org/10.1016/0021-9517\(92\)90054-L](http://dx.doi.org/10.1016/0021-9517(92)90054-L)
21. Koc SN, Gurdag G, Geissler S and Muhler M. Effect of nickel, lanthanum, and Yttrium addition to magnesium molybdate catalysts on the catalytic activity for oxidative dehydrogenation. *Industrial & Engineering Chemistry Research*. 2004; 52(6):2376-2381. <http://dx.doi.org/10.1021/ie030741j>
22. Brito JL, Laine J and Pratt KC. Temperature-programmed reduction of Ni-Mo oxide. *Journal of Materials Science*. 1989; 24(2):425-431. <http://dx.doi.org/10.1007/BF01107422>
23. Brito J and Laine J. Characterization of supported MoO<sub>3</sub> by temperature-programmed reduction. *Polyhedron*. 1986; 5(1-2):179-182. [http://dx.doi.org/10.1016/S0277-5387\(00\)84904-9](http://dx.doi.org/10.1016/S0277-5387(00)84904-9)